ICAS PAPER
No. 72 – 50

NOISE CONTROL TECHNOLOGY FOR
JET-POWERED STOL VEHICLES

by

Harvey H. Hubbard, Head, Acoustics Branch, Control Section,
David Chestnutt, Aerospace Technologist, and Domenic J. Maglieri,
Head, Aircraft Noise, NASA Langley Research Center, Hampton, Va., USA

The Eighth Congress of the International Council of the Aeronautical Sciences

INTERNATIONAAL CONGRESCENTRUM RAI-AMSTERDAM, THE NETHERLANDS
AUGUST 28 TO SEPTEMBER 2, 1972

Price: 3. Dfl.

NOISE CONTROL TECHNOLOGY FOR JET-POWERED STOL VEHICLES

Harvey H. Hubbard, David Chestnutt, and Domenic J. Maglieri
NASA Langley Research Center
Hampton, Virginia, U.S.A.

Introduction

In discussing noise control technology, it is important first to define the types of flight vehicles involved and the nature of the system in which they will operate. The first figure shows a sketch of a proposed STOL aircraft. In size, shape, range, speed, and weight it will resemble many of today's medium range jet transports. It does, however, differ markedly in the way its powerplants are integrated into the airframe and this is pertinent to the main discussions of this paper. It is significant that these vehicles will have an integrated lift propulsion system which provides more lift, a higher thrust-to-weight ratio, and shorter take-off and landing distances than current jet transports.(1-4)

The manner in which STOL vehicles are proposed to operate is indicated in Figure 2. In the figure are sketches showing the relative runway dimensions and the proposed landing-approach and take-off-climbout profiles for a STOL aircraft operation compared to CTOL. It can be seen that the STOL aircraft will have a markedly shorter ground run; and will climb out from the airport and will make its approach to the airport at steeper angles. The STOL system is expected also to operate in close proximity to built-up residential and commercial areas, and there is thus a requirement for acceptable noise characteristics.

Noise Goals

A noise goal of 95 EPNdB at 152 m has been put forth and has served as a guideline for configuration studies to date. A comparison of the estimated ground-noise contours for the proposed STOL aircraft and a current CTOL aircraft of comparable range is given in Figure 3. In the figure the relative runway dimensions are indicated by superposition, and the associated ground-noise contour for 95 EPNdB is shown for each system. It can be seen that the STOL aircraft-noise contour closes in a much shorter distance and encompasses a much smaller area than the comparable CTOL noise contour. In fact, it can be seen that the STOL noise contours can be contained within the boundaries of a conventional airport.

A further comparison of the noise characteristics of the two types of aircraft is given in Figure 4. Effective perceived noise levels as a function of maximum gross weight are shown as individual data points for several current airplanes. Also included on the figure as a solid line are the noise certification values specified by Federal Aviation Regulation 36.(5) The dashed line of the figure indicates the goal proposed in the recent Civil Aviation Research and Development (CARD) study for the 1981 time period.(6) This CARD study goal calls for approximately a 10-EPNdB reduction in the noise certification levels. Also shown on the figure is a cross-hatched area at the appropriate gross weight to indicate how the proposed STOL vehicles will compare. The goals for the STOL aircraft are near the bottoms of the diagrams and are thus seen to be consistent with the long-range goals for CTOL as put forth in the CARD study.

In order to compare more directly the noise goal for proposed STOL vehicles with the current FAR 36 levels, the data of Figure 5, from Reference 4, are presented. Perceived noise-level values are shown for three sideline situations. The left-hand bar represents present noise regulations for CTOL at 640 m. The middle bar represents the same regulation interpolated to a distance of 152 m and the right-hand bar represents the current STOL noise goals also at 152 m. Thus, the latter two bars are directly comparable and suggest that the noise-level goals for STOL represent approximately a 30-PNdB reduction at the source compared to those for the current STOL noise regulation. Such a sizable reduction in noise levels requires the effective use of noise-reduction technology. The problem of accomplishing such a noise reduction is difficult enough for conventional aircraft powerplants but may be aggravated because of the requirement for close integration of the powerplant with the lift-producing system of the aircraft.

Propulsion System Configurations

Figure 6 contains sketches of several integrated lift propulsion system concepts that are currently under study. The top-left sketch represents an externally blown flap in which the engine exhaust is directed toward a turning flap arrangement at the rear of the wing. External blowing can also be accomplished by placing the engine in such a way as to exhaust over the upper surface of the wing, and this is indicated schematically in the upper right-hand sketch. Other concepts which are generally more sophisticated in nature and require more complex hardware configurations are those at the bottom of the chart. The lower left-hand figure represents an augmenter wing configuration in which the engine exhaust flow is ducted first into the wing and then out of a wing slot into a flap augmenter system. The lower right-hand sketch represents an internally blown flap arrangement whereby the internally ducted engine airflow is exhausted over a shielding flap. The above concepts are at the present time in various stages of development and thus no attempt will be made to provide direct comparison evaluations. It is known, however, that the basic engine cycle requirements differ from one of these configurations to the other and thus entirely new engine developments can be anticipated.

Figure 7 serves to characterize the required engine cycles for the different integrated lift propulsion systems. Fan pressure ratio and exhaust velocity are shown as a function of engine bypass ratio. It can be seen that both the fan pressure ratio and the engine exit velocity decrease markedly as a function of bypass ratio. As indicated by the hatched areas, the preferred operating range for the augmenter wing and IBF concepts involve relatively high fan pressure ratios, and low engine bypass ratios, whereas the relatively low fan pressure ratios and high engine bypass

ratios are being considered for the EBF and upper surface blowing configurations. The close integration of the engine with the airframe in order to provide lift augmentation provides sources of noise as indicated in Figure 8.

The schematic diagrams of Figure 8 indicate the noise sources for a conventional fan engine at the left and those for an integrated lift propulsion system involving a fan engine at the right.(1) At the bottom of the figure are diagrams illustrating the nature of the associated noise spectra. The conventional fan engine has noise sources both external to the engine and internal to the engine, and the main directions of noise radiation are indicated. In this type of engine the noise spectra contain discrete frequency components from the rotating machinery sources and broad band noise due mainly to the jet exhaust.

The lift augmentation system has the noise sources indicated for the basic engine plus the noise of the engine exhaust interaction with the wing and turning flap components. The associated noise spectra are similar to those for the basic engine except that a substantial amount of interaction noise is observed and this is especially intense at the lower frequencies. Noise control of a STOL powerplant thus involves those technology items which relate to the basic engine plus those which relate to the wing and flap mechanisms.

Basic Engine Noise Sources

The data of Figures 9 through 12 relate to the noise generation by the basic fan engine and illustrate approaches to control of both internally and externally generated noise. The fan is a major source of internally generated noise and a summary of fan noise data is given in Figure 9(4) in which the maximum sideline noise levels are shown as a function of fan pressure ratio. The data shown are from families of research fans and some fan engines. It can be seen that a wide range of noise levels is associated with the fan component depending on its configuration and operating condition. Significant factors are fan pressure ratio, number of stages, tip speed, component spacing, blade-vane number, and reflection considerations. The lowest noise levels are associated with single stage, low-tip-speed machines operating at the lower fan pressure ratios.

Source considerations alone are not adequate for meeting the STOL noise goal of 95 EPNdB and hence additional noise-control approaches must be considered. One of these involves the use of acoustic duct liners, and the range of noise levels obtainable is indicated by the stippled area. The manner in which such treatment might be applied to a fan engine is illustrated in Figure 10.(3) This is a sectional view of the engine and the dark shaded areas are those in which absorptive materials would be placed both for fore and aft noise reduction. Although such materials have been demonstrated to be effective in noise control, there may in some cases be excessive weight, volume, or aerodynamic losses involved.(7)

An alternative method for inlet noise control is illustrated in Figure 11. Sketches are shown of three different concepts of hardware arrangements to accomplish inlet choking. The main objective for inlet choking is to provide a localized region of high Mach number flow ahead of the noise producing elements of the engine in order to substantially impede noise propagation in the direction against the flow. The device on the left represents a translating center body in which the choked flow occurs in the vicinity of the minimum area. Other minimum area concepts are shown by the center sketch which involves translating airfoil-shaped vanes and the sketch on the right which involves thickened or rotating inlet guide vanes. Considerable effort is underway to evaluate these concepts from a performance standpoint.

The jet is a major source of externally generated noise, and jet velocity is the most powerful factor in noise generation. The jet noise situation for a variety of jet engines is illustrated in Figure 12.(1) The hatched region represents a large number of measurements from engines, and these have been normalized to the same thrust level. It can be seen that the noise levels are relatively high at the higher velocities and reduce substantially as jet exhaust velocity is reduced. At the top of the figure are shown sketches suggesting the kinds of jet engines represented by the different velocity regimes. The turbojet engines are represented by the data at the far right of the curve and the high bypass ratio fan engines at the extreme left of the curve. The high bypass ratio engines have been designed to take advantage of the beneficial effects of reduced velocity.

An important consideration in jet engine noise is the fact that at the lower velocities there appears to be a significant amount of noise in excess of that attributed to the jet mixing phenomena. This suggests the possibility of the effectiveness of tailpipe acoustic treatment since this additional noise is believed to arise from phenomena inside of the engine. Although exhaust noise suppressors may be useful at high velocities, effective suppressors have not been developed for the low velocity range.

Jet-Surface Interaction Noise

Jet-surface interaction noise arises from the various interactions of surfaces placed in the vicinity of the jet engine exhaust in the process of integrating the engine into the airframe. Interaction noise is sensitive to geometry and flow conditions and thus its relative importance varies from one configuration to another.

Externally Blown

An indication of noise level increases due to interaction effects is given in Figure 13.(8) The sound pressure levels are shown as a function of frequency for a test arrangement having a wing plus turning flap, and a free fan jet exhaust for comparison. The spectra contain both broad band and discrete tone components. It can be seen that the most obvious change in the noise spectrum due to surface interactions is at the lower frequencies which are intensified by as much as 20 dB. The significance of this low-frequency noise and associated vibrations has not as yet been evaluated in human response.

The sources of interaction noise are at present not well defined, particularly for the complex

turning flap configurations of interest. An attempt is made in Figure 14, however, to identify some possible noise sources for the type of configuration of interest for externally blown flaps.[4] In addition to the internal and external jet noise, there are leading- and trailing-edge noise sources for each of the flow turning elements and scrubbing or impingement noise on some of the larger scale surfaces.

Some possible mechanisms of generation for such interaction noises are given in Figure 15. Interaction noise results from the interruption of the free mixing inflow streamlines due to the presence of a solid surface such as a wing. Other sources are the scrubbing action of the flow along the surface, and inflow turbulence which induces fluctuating lift forces at the leading edge of the airfoil. Surface impingement in some cases results in a pattern of correlated fluctuating pressures on the airfoil surfaces and these result in acoustic radiation to the far field. Another source of noise is the trailing-edge discontinuity which results in an abrupt impedance change for the flow as it leaves the airfoil. Because of the significance of the details of the flow on or near the impinged surfaces, there is considerable interest in the possibility of changing the character of the flow and thus beneficially affecting the noise radiation. This has led to a series of studies of the effects of airfoil surface treatment.[9]

Significant factors in the generation of flow interaction noise are indicated in Figure 16 as the wing flap geometry including airfoil chord lengths, thicknesses, span lengths, and locations relative to the engine exhaust; the velocity and turbulence level of the impinging jet flow, and the turning angles of the flow.[4] Although none of these factors have been completely evaluated, an attempt will be made in succeeding figures to indicate some of their effects on the radiated noise.

Figure 17 illustrates the effect of impingement velocity on the overall noise levels from an externally blown flap configuration compared to similar noise level data for the nozzle alone.[4] It can be seen that the noise levels increase markedly as the velocity increases and the flap noise levels are markedly higher than for the nozzle alone. Furthermore, the slopes of the two curves are different. The data for the nozzle alone tend to follow the familiar eighth power law, whereas the flap data tend to follow a sixth power law. Since the flap impingement velocity has such a significant effect on the radiated noise, there is considerable interest in procedures for reducing the velocity values.

One possible noise control procedure for an externally blown flap arrangement involves the use of velocity decay nozzles to substantially alter the mean flow velocity patterns in the region of the flap surfaces. The resulting velocity patterns obtained by means of this approach are illustrated in Figure 18.[10] The solid curve represents the ratio of local velocity to maximum jet center-line velocity at various axial distances from the nozzle for a circular jet. The dashed curve represents similar velocity data for a segmented nozzle which is designed to increase the rate of mixing of the primary flow with the ambient air. This results in lower values of local mean flow velocity in the vicinity of the impinged surfaces. This approach is a valid one for noise reductions due to flow impingement; however, there is a need for effective noise control procedures for the nozzles themselves.

Jet noise levels can be adversely affected by the presence of a surface such as a wing or turning flap, and the effects are a function of the relative locations of the surface. These effects are illustrated in Figures 19 and 20 (from unpublished work by D. Chestnutt, W. L. Copeland, and L. R. Clark). Figure 19 indicates the relative noise levels measured at 90° to the jet axis for a jet in the presence of a straight and a curved surface compared to the case of the jet alone. It can be seen that the noise levels are higher than for the jet alone for a range of radial distances. Similar results are given in Figure 20 for a range of axial separation distances. It thus follows that the relative locations of the engine and the wing-flap surfaces are important and are a possible means for noise control.

Flap turning angle also has significant effects as indicated by the data from a model setup of an externally blown flap in Figure 21.[4] Sound pressure levels are shown as a function of frequency for the nozzle alone as a baseline for comparison and for flap configurations from 0° to 60°. The net result is that the observed flap noise levels exceed those of the basic bypass nozzle by a significant amount at all frequencies and particularly at the lower frequencies. Increases in noise levels are seen to be associated with an increase in the flow turning angle.

Upper Surface Blowing

Because of the observation that flow turning by flaps is a noisy process, the question arises as to whether or not a quieter means of flow turning might be used. This has led to a renewed interest in flaps in which the flow to be turned is attached to the upper surface of the airfoil and turns because of the coanda principle. Some example noise radiation pattern results are given in Figure 22 in which similar noise level data are compared for lower and upper surface blowing.[4] The solid curve relates to a circular jet and external blown flap arrangement, whereas the dashed curve is for an upper surface blowing configuration with a slot nozzle of equivalent area. It can be seen that the latter configuration generates noise levels which are generally lower at all azimuth angles and particularly in the downward direction.

The noise sources in an upper surface blowing configuration can be identified with the aid of Figure 23. They include the internal disturbance, the scrubbing of the attached flow on the flap, the trailing edge of the flap, and the primary and secondary jet mixing regions.

In many, if not all, turning flap configurations, the airfoil trailing edges may be important noise sources. The radiation pattern due to airflow over the trailing edge of a solid surface is given in the central sketch of Figure 24.[11] In some respects the pattern resembles that of a dipole source and the noise radiated follows approximately a sixth power law of velocity. The introduction of an impedance gradient in the vicinity of the trailing edge as indicated schematically in the lower

right-hand sketch is effective in markedly reducing the radiated noise. This result has intensified interest in the possible use of porous edges for airfoil noise control.

Concluding Remarks

The material of this paper constitutes a brief progress report on the problem of community noise control for jet-powered STOL vehicles. Noise goals have been discussed along with noise control approaches for meeting these goals. Such considerations as the basic engine cycle, the concepts of engine-airframe integration, and the details of the lift augmentation system are identified as being significant in noise control. Needs are cited for a better understanding of the noise sources and the physical mechanisms, and the manner in which humans respond to low-frequency noise and vibration stimuli. Other factors which must be adequately considered to provide a useful STOL vehicle design are the noise and vibration environments of the interior spaces and the sonic fatigue of the airframe, particularly the flap structure.

References

1. NASA Aircraft Safety and Operating Problems. A Conference held at the Langley Research Center, Hampton, Virginia, May 4-6, 1971. NASA SP-270, Vol. I.

2. Vehicle Technology for Civil Aviation — The Seventies and Beyond. A Conference held at the Langley Research Center, Hampton, Virginia, November 2-4, 1971. NASA SP-292.

3. Kramer, James J., Chestnutt, David, Krejsa, Eugene A., Lucas, James G., and Rice, Edward J.: Noise Reduction. Presented at Conference on Aircraft Propulsion, NASA Lewis Research Center, Cleveland, Ohio, November 18-19, 1970. NASA SP-259, pp. 169-209.

4. Aircraft Engine Noise Reduction. NASA Lewis Research Center, Cleveland, Ohio, May 16-17, 1972. NASA SP-311, 1972.

5. Anon.: Noise Standards: Aircraft Type Certification. Federal Register, Vol. 34, No. 221, November 18, 1969, pp. 18364-18379.

6. Civil Aviation Research and Development Policy Study. Joint DOT-NASA, Washington, D.C., March 1971, NASA SP-265.

7. Progress of NASA Research Relating to Noise Alleviation of Large Subsonic Jet Aircraft. A Conference held at the NASA Langley Research Center, Hampton, Virginia, October 8-19, 1968.

8. Ganger, T. G.: Results of Prop-Fan/STOL Wing Acoustics Tests. Prepared by Hamilton Standard Division of United Aircraft Corp. NASA CR 111956, July 29, 1971.

9. Hayden, Richard E.: Noise From Interaction of Flow With Rigid Surfaces: A Review of Current Status of Prediction Techniques. NASA CR-2126, 1972.

10. Groesbeck, D. E., von Glahn, U. H., and Huff, R. G.: Peak Axial-Velocity Decay With Multi-Element Rectangular and Triangular Nozzles. NASA TM X-68047, March 1972.

11. Hayden, R. E.: Sound Generation by Turbulent Wall Jet Flow Over a Trailing Edge. Master's Thesis, University of Purdue, August 1969.

Figure 1. Proposed jet-powered STOL vehicle.

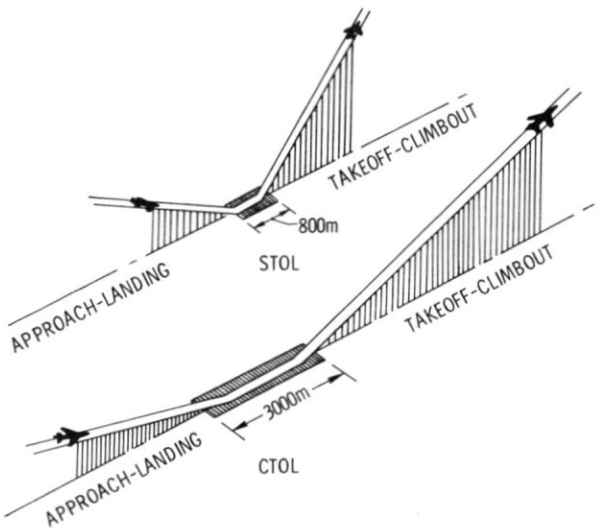

Figure 2. Comparison between landing approach and take-off-climbout profiles for STOL and CTOL vehicles.

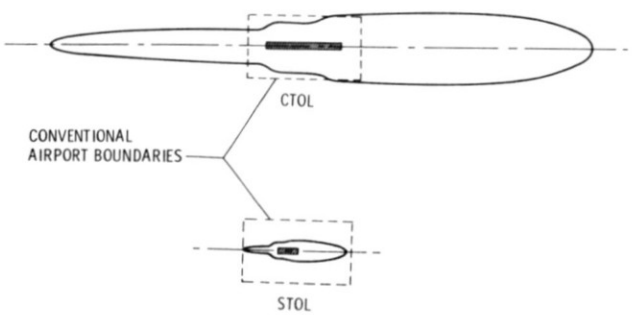

Figure 3. Comparison of ground-noise exposure areas for STOL and CTOL vehicles.

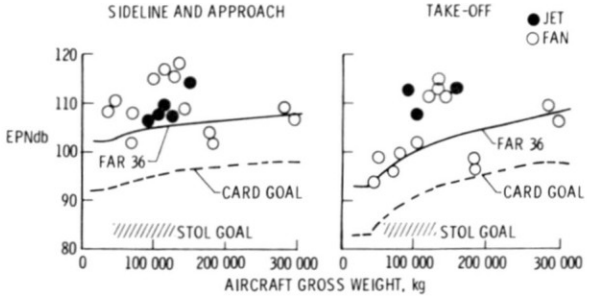

Figure 4. External noise goals for future STOL and CTOL vehicles.

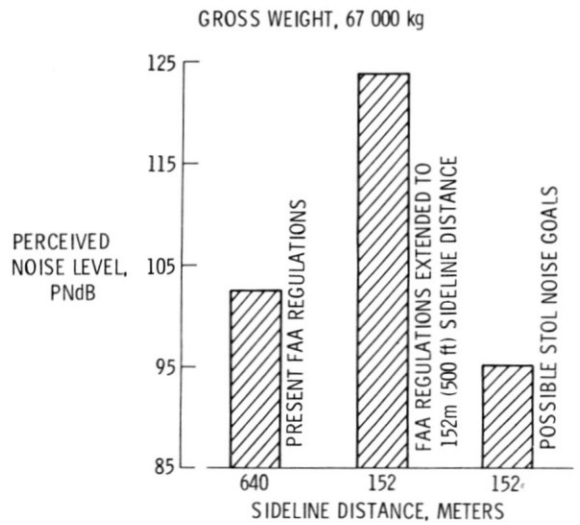

Figure 5. Comparison of STOL and CTOL noise goals.

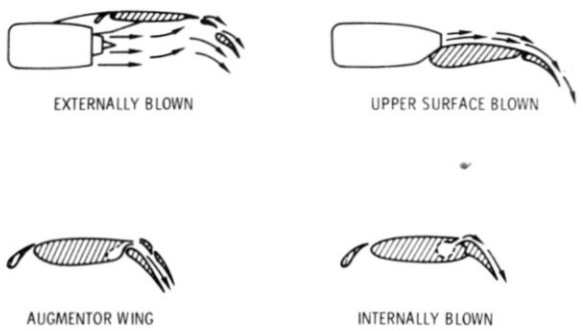

Figure 6. Integrated lift-propulsion concepts for jet-powered STOL vehicles.

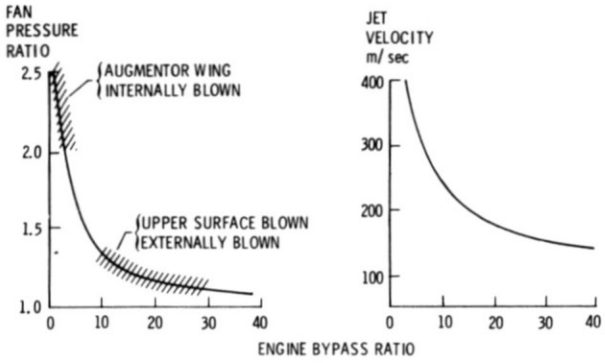

Figure 7. Relationships between fan engine bypass ratio, fan pressure ratio, and jet exhaust velocity.

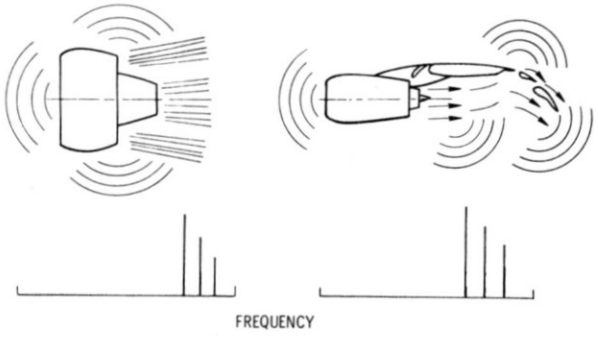

Figure 8. Schematic illustrations of the noise source locations and the characteristic spectra of conventional and blown flap propulsion systems.

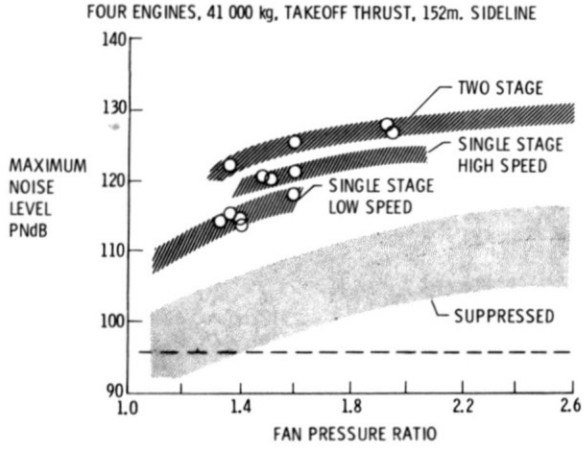

Figure 9. Maximum sideline fan noise levels as a function of fan pressure ratio.

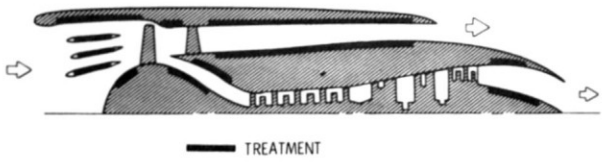

Figure 10. Schematic illustration of the areas of possible application of acoustical duct treatment in a high bypass ratio fan engine.

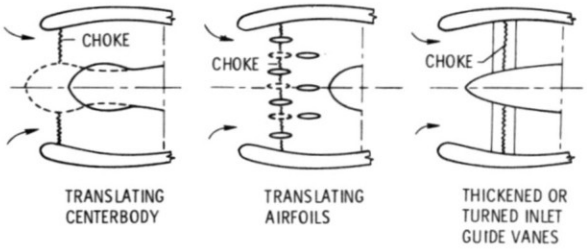

Figure 11. Three possible configurations for creating choked flow in the inlet of a fan engine.

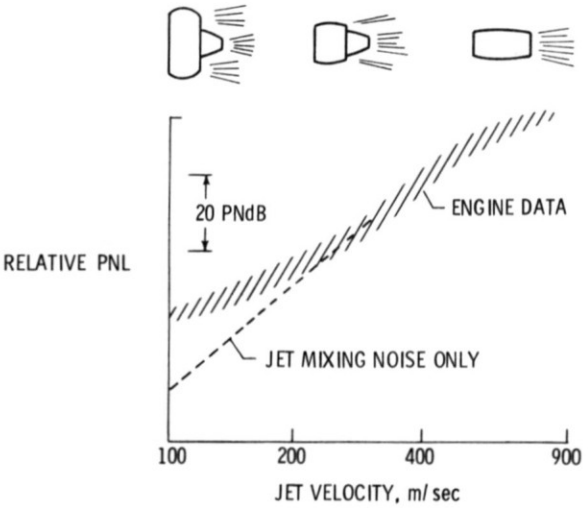

Figure 12. Effects of jet engine exhaust velocity on the relative perceived sideline noise level for a constant thrust.

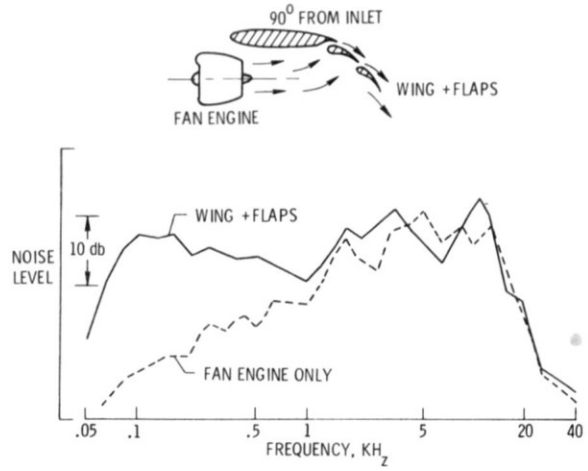

Figure 13. Comparison of noise spectra for a fan jet engine with and without an externally blown flap.

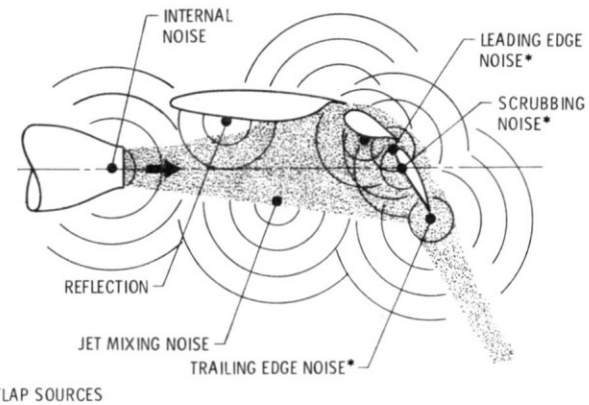

Figure 14. Schematic illustrations of the locations of externally blown flap noise sources.

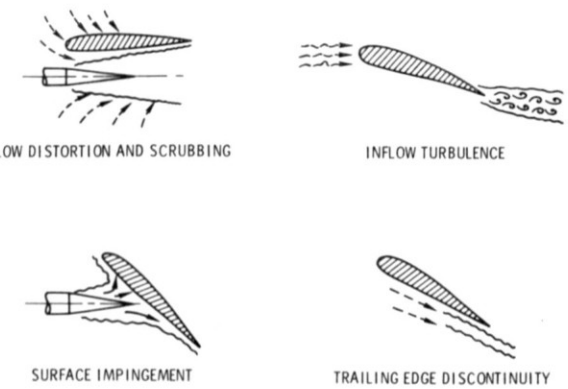

Figure 15. Schematic illustrations of flow interaction noise sources.

- IMPINGMENT VELOCITY
- WING-FLAP GEOMETRY
- FLAP TURNING ANGLE
- TURBULENCE LEVEL

Figure 16. Significant factors in flow interaction noise generation.

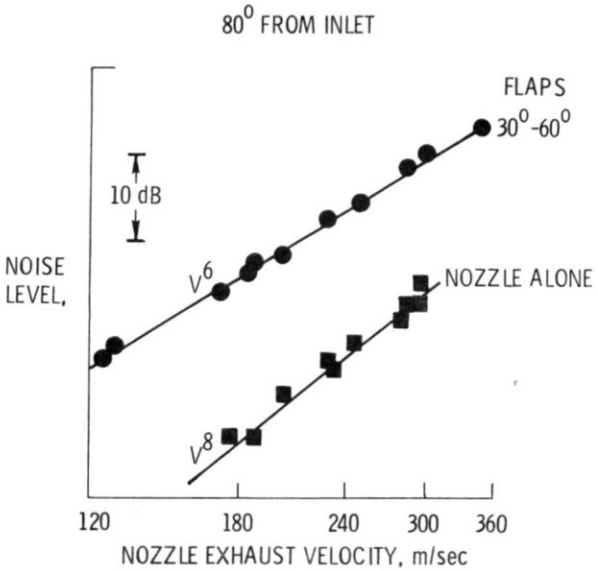

Figure 17. Overall noise level as a function of nozzle exhaust velocity for an externally blown flap compared to the nozzle alone.

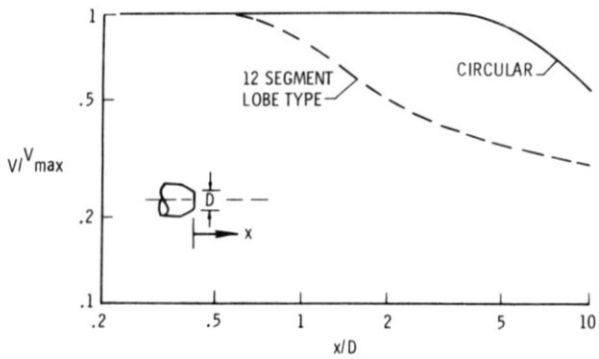

Figure 18. Axial velocity distributions for two different nozzle configurations.

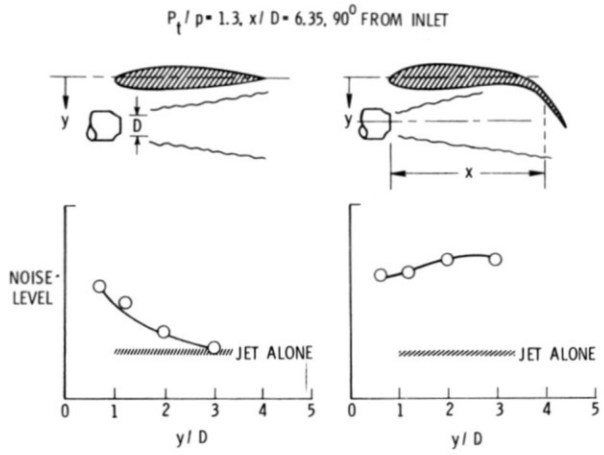

Figure 19. Effects of radial distance from the wing surface on the flow-surface interaction noise from a jet.

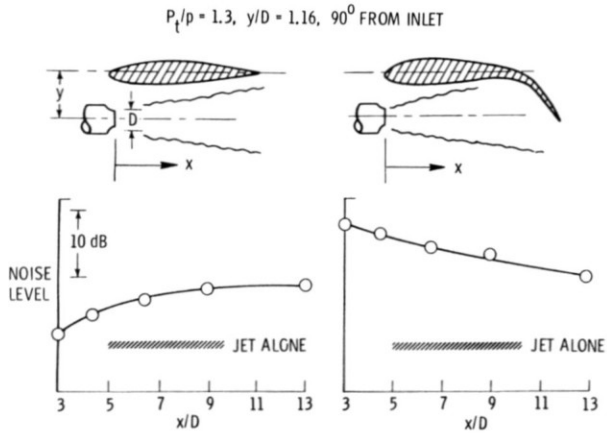

Figure 20. Effects of axial distance from the flap surface on the flow-surface interaction noise from a jet.

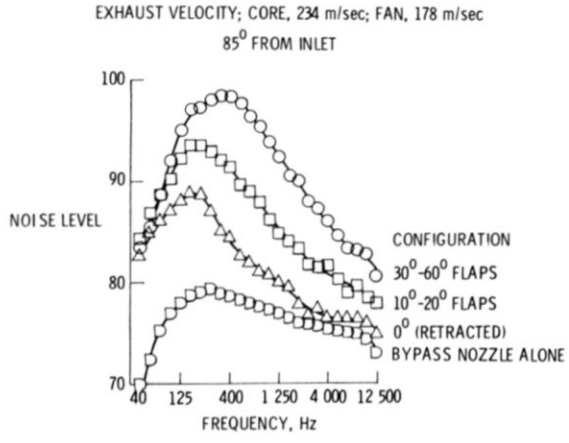

Figure 21. Effects of flow turning angle on the noise spectra from an externally blown flap.

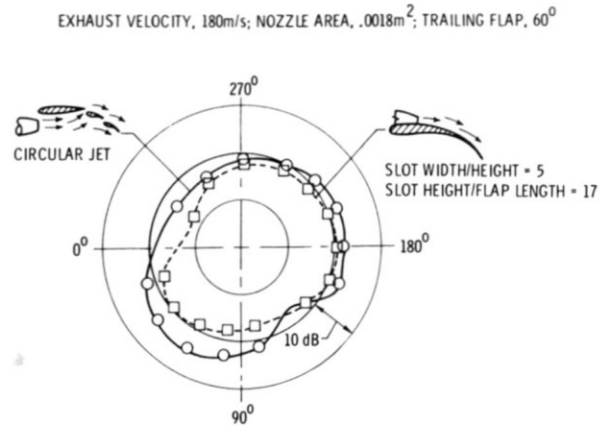

Figure 22. Comparison of the overall noise radiation patterns from lower and upper surface blown flaps.

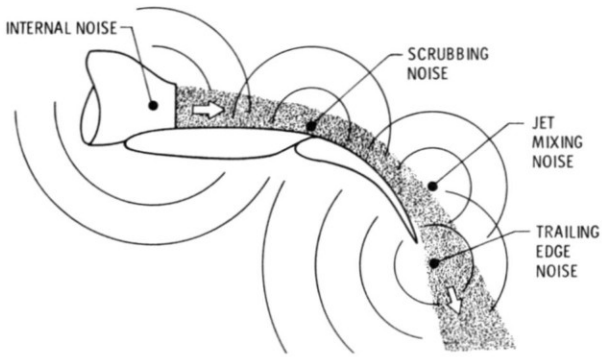

Figure 23. Schematic illustration of locations of noise sources for upper surface blown configurations.

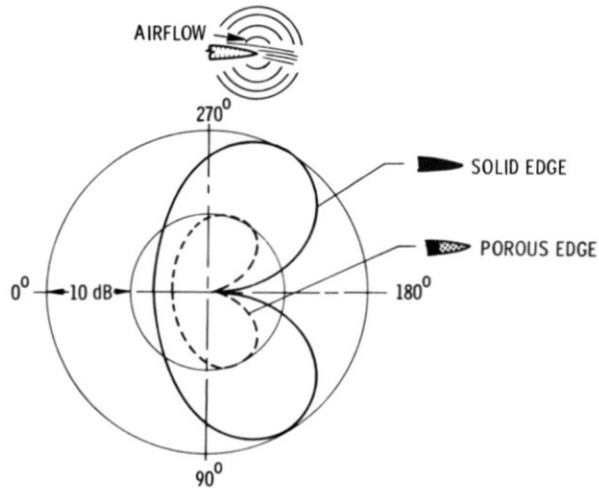

Figure 24. Trailing-edge noise radiation patterns.